

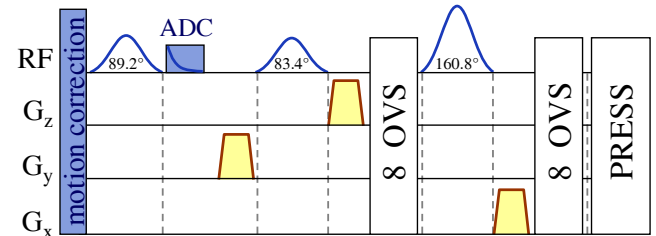
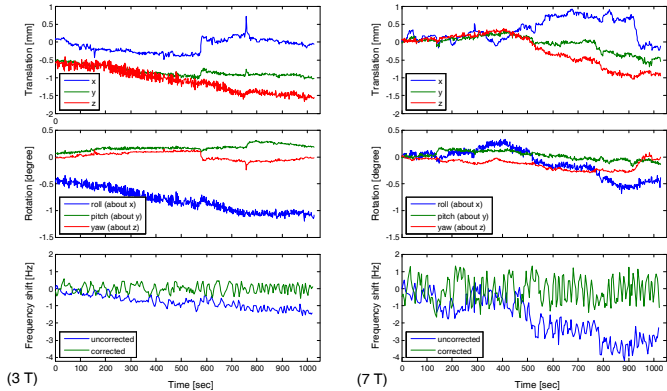
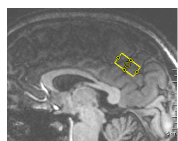
Adaptive motion correction of single-voxel spectroscopy with real-time frequency correction at 3 T and 7 T

Christian Labadie¹, Thomas Siegert¹, Enrico Reimer¹, Maria Guidi¹, Miguel Martinez-Maestro¹, Harald E. Möller¹, Robert Turner¹, and Jessica Schulz¹
¹Max Planck Institute for Human Cognitive and Brain Sciences, Leipzig, Germany

Target audience – Proton spectroscopy of the brain.

Purpose – In proton single-voxel spectroscopy (SVS), the low signal to noise ratio of metabolites is improved by coherently averaging high number of scans. During such long acquisitions, the inevitable head motion affects the localization of the voxel of interest (VOI), leading to signal contamination from neighboring tissues. To improve the tissue specificity, considerable efforts have been made to assess head motion and to adapt in real-time the VOI localization [1], either by acquiring navigators [2,3] or by externally monitoring head motion [4–7]. Displacement of the head slightly affects the field homogeneity with deteriorating consequences on the phase of the signal [3,8]. Furthermore, long acquisitions are affected by magnetic field drifts of few Hz per hour [8,9], that may vary depending on the helium cooling of super-conducting magnet [10] or the demand on gradient systems. This has been addressed by determining the spatial variation of the phase and updating shim values [2,3,7], principally along the three axes. Following a real-time shim update, the frequency is estimated from the water signal, either with a navigator [2,3] or retrospectively from the phase of the water peak [4,6,7]. In this abstract, we present a simplified approach consisting of fetching the current position of the head before each scan using an embedded set of three cameras placed near the head coil [11], and determining the frequency from the transverse magnetization of the water protons after the first frequency selective 90° saturation pulse of the WET water suppression scheme [12]. This method does not modify the timing of the PRESS sequence in which it was implemented, and allows adapting localization and frequency in real-time before starting the second water saturation pulse and the outer-volume suppression (OVS) slabs.

Methods – Embedded tracking: Adaptive motion correction was performed in real-time at each scan before the WET module of PRESS sequence using the XPace library, kindly provided by M. Zaitsev, M. Herbst and J. Maclare [1,13] and a home-built optical tracking system [11]. Scanners: Siemens (Erlangen) TIM Trio 3 T with the lower part of a 12-channel head coil (upper part removed to accommodate three cameras), and investigational 7 T with an 8-channel coil. Real-time frequency assessment: Following the first 90° water selective saturation pulse, an FID was collected at TE 1 ms with 512 points of 20 μ s dwell-time. Initial points were skipped to avoid effects related to switching the receiver. ADC points were analyzed pair-wise to determine a reference phase for each channel, to which subsequent ADCs were compared to determine a frequency offset. PRESS sequence: After real-time processing of the ADC (ca. 10 ms) the gradient spoiler is played, and the rest of the WET [12], OVS, and PRESS selection, which are performed with an adapted frequency, VOI position and rotation matrix.



Acquisition and processing: After receiving informed consent from a 23 year old woman volunteer, a 2 mL VOI (10x10x20 mm³) was placed in parietal gray matter and measured at 3 T and 7 T after performing an automatic shim based on a double-echo fieldmap (Siemens WIP452). For comparison, 256 averages were acquired interleaved with and without adaptive motion/frequency correction (TE 30 ms, TR 2 s, 4 pre-scans, 1024 points, 2800 Hz bandwidth, 16-step exor-phase cycling). LCMModel processing [14] was performed with an in vitro basis-set at 3 T and a gamma simulated basis-set at 7 T [15].

	3 T		7 T	
	corrected	uncorrected	corrected	Uncorrected
Cre %SD	5	5	3	4
Glu %SD	10	10	10	11
mI %SD	11	9	10	11
NAA %SD	6	6	3	3
NAAG %SD	37	31	12	15
GPC+PCh %SD	9	8	6	7
Glx %SD	9	4	13	15
FWHM / ppm	0.022	0.033	0.037	0.037

Full-width at half-maximum (FWHM) and Cramer-Rao lower bound (CRLB, in pct. standard deviation) of LCMModel estimations of metabolite concentration: creatine (Cre), glutamate (Glu), myo-inositol (mI), N-acetyl aspartate (NAA), NAA-glutamate (NAAG), total choline (GPC+PCh), glutamine+Glu (Glx).

Results and Discussion – The Figure displays translations (top), rotations (middle) and frequency shifts (bottom) observed at 3 T (left) and 7 T. During these long measurements (TA 17 min 12 s) involuntary head movements were observed, which are effectively corrected with the proposed method (validation performed with 3D imaging [11]). A frequency shift (uncorrected, blue curve) is observed at both fields, and was successfully corrected (stable about 0 Hz, green curve). The Table presents a comparison of LCMModel results. At 3 T, the FWHM slightly improved with adaptive correction of motion and frequency, but the CRLB increased for mI, NAAG, choline, and Glx. At 7 T, CRLBs improved with adaptive correction (except for NAA) but the FWHM remained unchanged. These results confirm the presence of a frequency shift [9] at 3 T and 7 T, and of head motion resulting from relaxing the head neck, tilting of the head, or swallowing. Abrupt motions or frequency changes could be detected, skipped and repeated at run time. We note that our method does not update the shim, which could further improve the adaptive correction [2,7].

References – [1] Maclare, MRM 2013, [10.1002/mrm.24314](https://doi.org/10.1002/mrm.24314). [2] Keating, MRM 2010, [10.1002/mrm.22448](https://doi.org/10.1002/mrm.22448). [3] Hess, MRM 2011, [10.1002/mrm.22805](https://doi.org/10.1002/mrm.22805). [4] Zaitsev, NMRB 2010, [10.1002/nmr.1469](https://doi.org/10.1002/nmr.1469). [5] Andrews-Shigaki, JMRI 2011, [10.1002/jmri.22467](https://doi.org/10.1002/jmri.22467). [6] Lange, MRM 2012, [10.1002/mrm.23136](https://doi.org/10.1002/mrm.23136). [7] Keating, MRM 2012, [10.1002/mrm.24129](https://doi.org/10.1002/mrm.24129). [8] Ebel, MRM 2005, [10.1002/mrm.20367](https://doi.org/10.1002/mrm.20367). [9] Tal, MRM 2013, [10.1002/mrm.24536](https://doi.org/10.1002/mrm.24536). [10] Jehenson, JMR 1990, [10.1016/0022-2364\(90\)90133-T](https://doi.org/10.1016/0022-2364(90)90133-T). [11] Schulz, Magma 2012, [10.1007/s10334-012-0320-0](https://doi.org/10.1007/s10334-012-0320-0). [12] Ogg, JMR 1994, [10.1006/jmra.1994.1048](https://doi.org/10.1006/jmra.1994.1048). [13] Zaitsev, Neuroimage 2006, [10.1016/j.neuroimage.2006.01.039](https://doi.org/10.1016/j.neuroimage.2006.01.039). [14] Provencher, MRM 1993, [10.1002/mrm.1910300604](https://doi.org/10.1002/mrm.1910300604). [15] Smith, JMR 1994, [doi:10.1006/jmra.1994.1008](https://doi.org/10.1006/jmra.1994.1008).

Acknowledgement – Funded through the Helmholtz Alliance ICEMED, the EXIST program, and the Marie Curie ITNs TRANSACT and HiMR.